JOURNAL OF CATALYSIS 147, 301–310 (1994)

The Effect of Chloride Ions on a Li^+–MgO Catalyst for the Oxidative Coupling of Methane

Jack H. Lunsford,[1] Paul G. Hinson, Michael P. Rosynek, Chunlei Shi, Mingting Xu, and Xueming Yang

Department of Chemistry, Texas A & M University, College Station, Texas 77843

Received October 5, 1993; revised January 3, 1994

At Cl/Li atomic ratios approaching unity, Li^+–MgO–Cl^- catalysts undergo a marked change in behavior with respect to the oxidative coupling of CH_4 to form C_2H_4 and C_2H_6 hydrocarbons. Most significant are the large C_2H_4/C_2H_6 ratios that may be obtained, primarily as a result of the enhanced activity for the oxidative dehydrogenation of C_2H_6. The presence of Cl^- ions at the appropriate level modifies the catalyst so that it no longer functions as a strongly basic oxide. In particular, the catalyst is not poisoned by CO_2, which normally dominates the kinetic behavior of a Li^+–MgO catalyst. The intrinsic activity for $CH_3\cdot$ radical generation over a properly chlorided Li^+–MgO catalyst is less than that of a normal catalyst, but after poisoning by CO_2, the activities of the two catalysts are comparable. At the typical reaction temperature of 650°C, chlorine is slowly lost from the catalyst, but this chlorine may be replaced by adding a small amount of HCl intermittently to the feed stream. At temperatures as low as 625°C, a CH_4 conversion of 29% and a C_{2+} selectivity of 60% may be achieved. © 1994 Academic Press, Inc.

INTRODUCTION

A practical goal in the oxidative coupling of methane is to produce high yields of ethylene. Ethane is the primary product of the reaction; however, in a single catalyst bed the oxidative dehydrogenation (OXD) reaction also occurs. It has been demonstrated by several investigators that the latter reaction is promoted by chlorine, either added directly to the catalyst or introduced into the reagent stream as HCl or an organic chloride (1–3).

Burch and co-workers (4–6) have carried out studies on the promotional effect of chlorine on the partial oxidation of methane over several catalytic materials. They found that the injection of pulses of gaseous chlorinated compounds over MnO_2, Li/MnO_2, Li/MgO, and Li/Sm_2O_3 increased the selectivity to ethane and ethylene for various periods of time. The addition of CH_2Cl_2 to a LiCl/MgO catalyst resulted in higher C_2H_4/C_2H_6 ratios. The total C_2 (C_2H_4 plus C_2H_6) production was essentially unchanged, suggesting that CH_2Cl_2 acts to promote the dehydrogenation of ethane. Otsuka *et al.* (7) found that a pulse of CH_3Cl passed over a Li/NiO catalyst increased the ethane selectivity for several hours.

Since chlorine is known to effect the dehydrogenation of C_2H_6 in the gas phase, it has been suspected that homogeneous reactions may be responsible for the large C_2H_4/C_2H_6 ratios that are observed in these chlorine-containing systems (2, 8). Burch *et al.* (6) found that CH_3Cl was ineffective in enhancing C_2H_4 selectivity, although HCl significantly promoted the conversion of ethane to ethylene in a gas phase process. A 1.5% HCl concentration in the feed was required to obtain ethylene yields, in a purely homogeneous reaction, similar to those obtained over a LiCl/MnO_2 catalyst. Increasing the postcatalytic volume did not have a positive effect on selectivity, indicating that homogeneous reactions in this region are not responsible for the enhanced C_2H_4/C_2H_6 ratios.

Burch *et al.* (4) have proposed that with alkali chloride–$MnCl_2$ catalysts, the improved C_2 selectivity results from the formation of a manganese oxychloride surface. Lambert and co-workers (9), using modified Mn_3O_4, have confirmed the positive effects of chlorine introduced via the gas phase or as KCl. The greater C_2 selectivity is attributed either to site modification or the formation of active chlorine radicals on the surface.

More recently, as a result of transient studies, Burch *et al.* (10) have concluded that at low concentrations (ca. 25 ppm), there is no detectable effect of gas phase chlorine. Rather, an important role of chlorine is to produce new sites that are particularly effective in the activation of ethane. Both HCl and Cl_2 at 1700 ppm inhibit the activation of CH_4 over Sm_2O_3, and they cause the C_2H_4/C_2H_6 ratio to *decrease*.

Thomas *et al.* (11) have examined a family of bismuth oxychlorides for catalytic activity in methane coupling. They reported CH_4 conversions up to 42% and C_2H_4/C_2H_6 ratios as great as 35. However, these materials generally lost activity within a few hours. They observed that the

---

[1] To whom correspondence should be addressed.

0021-9517/94 $6.00
Copyright © 1994 by Academic Press, Inc.
All rights of reproduction in any form reserved.

structures with the least labile chlorine were the most active for methane conversion, although this trend did not necessarily hold for C_2H_4/C_2H_6 ratios. Khan and Ruckenstein (12) found $BiOCl/Li_2CO_3/MgO$ materials to be active and selective catalysts. Neither BiOCl nor BiOCl/MgO were very effective, but the $BiOCl/Li_2CO_3/MgO$ catalyst gave 18% conversion and 83% selectivity after 5 h on stream. The C_2H_4/C_2H_6 ratio was 2.9. Temperature-programmed desorption (TPD) and X-ray photoelectron spectroscopy (XPS) results suggested that lithium helps stabilize the chlorine on the surface. Furthermore, the bismuth is believed to enhance C_2 selectivity.

The reported lifetimes of most chlorine-containing catalysts are relatively short. Burch *et al.* (6) observed deactivation in a few hours, in agreement with the report of Otsuka *et al.* (13), who found that several LiCl/transition metal oxides deactivated within 3 h at 750°C. The LiCl/NiO system deactivated in a relatively short period at 750°C, but at 640°C the catalyst was found to be stable for more than 20 h on stream.

Hinson *et al.* (14) found that a Li^+–MgO–Cl^- catalyst prepared via a sol–gel process was effective for periods up to 238 h. C_2 yields up to 20% and C_2H_4/C_2H_6 ratios of ca. 5 could be achieved at 640°C. At this temperature, the rate of chlorine loss from the catalyst was small. In a related study, Conway and Lunsford (3) found that the same catalyst was highly effective in the OXD of ethane at 650°C. Ethylene yields as great as 45% (65% C_2H_6 conversion and 69% C_2H_4 selectivity) were found. These results are consistent with the large C_2H_4/C_2H_6 ratios observed in the oxidative coupling reaction.

Ruckenstein and Khan (15) also have found that the addition of mixed alkali metal chlorides to MgO yielded stable catalysts that were active and selective for the oxidative coupling reaction. These catalysts gave C_2H_4/C_2H_6 ratios as great as 2.2. Based on benzoic acid titration and CO_2 desorption measurements, the authors concluded that these materials were highly basic, and that the residual chlorine species only enhanced the C_2 selectivity initially. This group also found that a Na^+–ZrO_2–Cl^- catalyst prepared by a sol–gel method was characterized by a CH_4 conversion of 14%, a C_2 selectivity of 77%, and a C_2H_4/C_2H_6 ratio of 3.3 after 30 h on stream at 750°C (16).

In the present study, the role of Cl^- ions in modifying the Li/MgO catalyst was evaluated in more detail by independently varying the concentration of Li^+ and Cl^- ions in the catalyst. It will be shown that the presence of Cl^- ions in a Cl/Li ratio of ≥ 0.9 has a dramatic effect on the nature of the active centers. With the addition of Cl^- ions, the intrinsic rate of CH_4 activation decreases, but the catalysts are also much less subject to poisoning by CO_2. Moreover, Cl^- ions inhibit extensive sintering of the catalysts. As a result, under normal operating conditions, the Li^+–MgO–Cl^- catalysts give greater CH_4 conversions than the conventional Li/MgO catalysts. Since the chlorided catalysts are not poisoned by CO_2, they are particularly well suited for a kinetic study. A previously developed model (17, 18) has been used to interpret the kinetic data. A related paper will provide additional information on catalyst characterization and will focus on the oxidative dehydrogenation of ethane.

EXPERIMENTAL

Catalyst Preparation

The catalysts that contained both Li^+ and Cl^- ions were prepared both by a sol–gel method and an aqueous slurry method. In the sol–gel method, the MgO was derived from the hydrolysis of a magnesium alkoxide, $Mg[-OCH_2CH_2CH(CH_3)_2]_2$, prepared according to a variation of a method described in the literature (19, 20). A catalyst consisting of $HgCl_2$ and CCl_4 was necessary to promote the reaction between magnesium metal and 3-methyl-1-butanol, and chlorine was introduced into the final product via this catalyst.

A typical sol–gel preparation was carried out using 4 g of Mg metal in a 500-ml, three-neck round bottom flask, equipped with a chilled-water condenser. The condenser was necessary to prevent loss of CCl_4. The system was flushed with N_2. After the Mg and the 3-methyl-1-butanol had been heated to 110–130°C, $HgCl_2$ and a few ml of CCl_4 were added. Following initiation of the reaction, CCl_4 was added as needed to sustain the reaction, and the remaining 3-methyl-1-butanol was added slowly. Typically, the reaction was complete within 1 h, but the solution remained another 2 h before lithium was added as $LiNO_3$.

Hydrolysis was achieved by passing a water-saturated stream of N_2 through the solution. Drying was carried out on a hotplate in an open beaker. This was sometimes followed by heating the catalyst in a vacuum oven at ca. 160°C. The dried material was ground to a powder and calcined at 500°C for several hours and then at 600–750°C for 10–16 h. This material was ground again and pressed into wafers, which were broken and sieved to 20/45 mesh. Finally, the catalyst was calcined a second time at 500°C and then at 750°C. Catalysts prepared by the sol–gel method are designated Li^+–MgO–Cl^- (SG).

In the slurry method, HCl was added slowly to a stirred aqueous slurry of MgO or $MgCO_3$ and $Mg(OH)_2$ at 40°C, and the mixture was stirred for several hours. Typically, Fisher MgO (light) was used; however, EM Science $4MgCO_3 \cdot Mg(OH)_2 \cdot 5H_2O$ also yielded a catalyst that gave high C_2H_4/C_4H_6 ratios. Fisher ACS certified MgO was not as effective a starting material. It appears that a MgO or $MgCO_3$ sample of low apparent density is needed.

The initial surface area of the MgO starting material is not a critical factor. An aqueous solution of $LiNO_3$ was then added to the slurry, and the water was evaporated while the slurry was stirred. The solid material was further dried in an oven and ground to a powder. Some of the preparations were calcined, reground, pressed into wafers, sieved to 20/45 mesh, and calcined a second time in manner similar to the catalysts derived from the sol–gel method. Other preparations were calcined only once. The second calcination did not appear to have any effect on the catalytic properties. The catalysts are designated Li^+–MgO–Cl^- (R), where R refers to the Cl/Li ratio. Unless stated otherwise, the Li/Mg atomic ratio was 0.3.

A conventional Li^+–MgO catalyst, without chloride ions, was prepared in the usual manner by adding Li_2CO_3 to a MgO slurry. The material was dried and calcined at 750°C for 16 h. The Li^+–MgO catalyst contained 5 wt% Li (atomic ratio of Li/Mg = 0.3). The initial compositions of all of the prepared catalysts are given in Table 1.

Reactor System

Reactions were carried out in both integral and differential modes. The integral reactor was constructed of a high purity alumina tube (Coors AD-998, 99.8% Al_2O_3) that was 19 mm i.d. at the large end and 3 mm i.d. at the small end. The catalyst was placed just above the section of the reactor where the diameter decreased; the gas flow was downward. The space above and below the catalyst was filled with alumina chips. A 6.4-mm o.d. alumina thermocouple well extended into the catalyst bed, along the axis of the reactor.

The differential reactor was constructed from an alumina tube having an i.d. of 6.4 mm. A second alumina tube of 6.2 mm o.d. and 3.0 mm i.d. was inserted to a point halfway along the length of the larger tube. The catalyst bed was supported on a layer of quartz wool, which rested on the top of the inner tube. Alumina chips were placed above the catalyst bed. A 3.2-mm o.d. fused-quartz thermocouple well extended down the central axis of the reactor to the top of the catalyst bed.

TABLE 1

Catalyst Composition

Sample	Li/Mg/Cl[a] atomic ratio
Li^+–MgO–Cl^- (0.3)	0.30/1.00/0.10
Li^+–MgO–Cl^- (0.7)	0.28/1.00/0.19
Li^+–MgO–Cl^- (0.9)	0.22/1.00/0.21
Li^+–MgO–Cl^- (1.0)	0.31/1.00/0.31
Li^+–MgO–Cl^- (SG)	0.27/1.00/0.27
Li^+–MgO	0.31/1.00

[a] Calcined samples.

The gases which consisted of 5% N_2 in He (Matheson), hydrocarbons (Matheson, ultrahigh purity) and O_2 (Matheson, extra dry) were introduced through mass flow controllers (MKS). The product stream was analyzed using a gas chromatograph (HP 5890A) with an integrator. A Porapak Q column was used to separate CO_2, C_2H_6, C_2H_4, C_3's, and C_4's; a 13X molecular sieve column was used to separate O_2, N_2, CH_4, and CO.

Sample Characterization

A postreactor water trap was used to collect the small amount of HCl produced during the catalytic reactions over the chlorided catalysts. The quantity of chloride in the solution was determined using a LaMotte chloride test kit. Bulk analysis for lithium and magnesium was by inductively coupled plasma (ICP) spectroscopy and for chloride by a gravimetric method (21).

X-ray diffraction was carried out using a Seifert–Scintag PAD V diffractometer. Because the chlorine-containing samples were hygroscopic, air-tight cells with Mylar windows were used. The samples were dried at 350°C and transferred to the cells inside a glove box purged with N_2.

The temperature-programmed desorption (TPD) of CO_2 from the catalysts was determiend using a thermal conductivity detector. A mass spectrometer attached to the system provided an identification of the desorbing gas. The samples were pretreated in He at 750°C for 1 h, cooled to 600°C, and exposed to CO_2 (Matheson, 99.8%) for 2 h. The catalysts were then cooled in CO_2 to 150°C, flushed with He, heated to 870°C at a rate of 16.5°C/min, and held at 870°C. As confirmed by mass spectrometry, the only evolved gas was CO_2.

RESULTS AND DISCUSSION

Catalytic Results

As pointed out previously (14) the coupling reaction over Li^+–MgO–Cl^- (SG) catalysts is characterized by favorable CH_4 conversions, good overall C_{2+} selectivities, and large C_2H_4/C_2H_6 ratios for long periods at 640°C. The results of Fig. 1a show that in the integral reactor, similar results were found over a Li^+–MgO–Cl^- (1.0) catalyst. Over a period of 160 h at 650°C, the C_2H_4/C_2H_6 ratio decreased from 4.1 to 2.7, while the total C_{2+} selectivity remained nearly constant. The level of CH_4 conversion decreased only 7%. It is generally observed for these catalysts that the C_2H_4 productivity decreases more rapidly than does the CH_4 conversion rate, while the total C_2 productivity remains nearly constant. By comaprison, over a comparable Li^+–MgO catalyst, the C_2H_4/C_2H_6 ratio would be ca. 0.7.

The gradual changes in catalytic results were accompa-

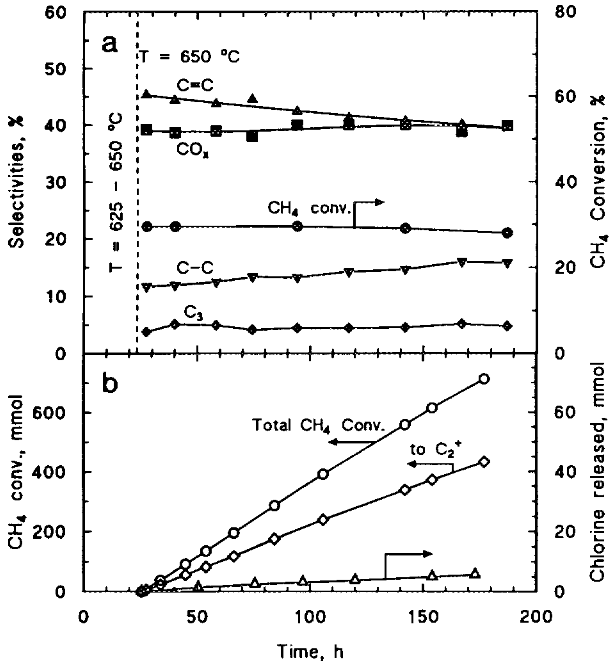

FIG. 1. (a) Variation in oxidative coupling of CH_4 over a Li^+–MgO–Cl^- (0.9) catalyst with time on stream: (●) CH_4 conversion; (▲) C_2H_4, (▼) C_2H_6, (◆) C_3, and (■) CO_x selectivities. (b) CH_4 conversion and chlorine released as a function of time on stream. The reaction was carried out over 6 g catalyst at partial pressures of 100 Torr CH_4 and 38 Torr O_2 at 50 ml min^{-1}.

nied by the loss of a small amount of the chlorine from the catalyst as HCl. Only trace amounts of CH_3Cl were observed in the product stream. We concluded earlier (3) that the loss of chlorine is associated with the production of water during the reaction. As indicated from the results of Fig. 1b, the ratio of moles of CH_4 converted to moles of chlorine released was 129, and the analogous ratio of C_{2+} formed to chlorine released was 78. Thus, if C_2H_4 is produced via chlorine-mediated gas phase reactions, the chain length for these radical reactions must be very long, considering the fact that only a fraction of the HCl would be converted to Cl.

Over a used Li^+–MgO–Cl^- (SG) catalyst, HCl was added to the inlet stream; the results are summarized in Table 2. The HCl was first introduced at a rate of 0.05 m mol h^{-1}, which corresponds to the rate of HCl release described in Fig. 1b. This amount of added HCl caused almost no change in the product distribution. After 20 h, the rate of HCl in the feed was increased to 0.21 mmol h^{-1}, which resulted in a slow decrease in the CO_2 selectivity and a parallel increase in the CO selectivity. Moreover, the C_2H_4/C_2H_6 ratio increased from 5 to 11. This might be interpreted as evidence for a gas phase reaction involving chlorine; however, when the introduction of HCl was stopped, the large C_2H_4/C_2H_6 ratio, as well as the CO productivity, remained at a high level for many hours. These results agree with those of Burch *et al.* (10) and suggest that it is the surface chlorine that is responsible for the large C_2H_4 productivity.

The effect of temperature on the catalytic properties of a Li^+–MgO–Cl^- (1.0) catalyst is shown in Fig. 2. One of the attractive features of this class of catalysts is that it reaches its optimum C_{2+} selectivity and C_2H_4/C_2H_6 ratio at a relatively low temperature, for an oxidative coupling reaction, of 625–650°C. At only 625°C, a C_{2+} selectivity of 60% was achieved at a conversion level of 29%, using

TABLE 2

Conversion and Selectivities of a Li^+–MgO–Cl^- (SG) Catalyst during HCl Co-Feed

Time on stream[a] (h)	HCl addition rate, (mmol h^{-1})	CH_4 conv. (%)	O_2 conv. (%)	Selectivities (%) C_2H_4	C_2H_6	CO_2	CO	C_{2+} yield (%)
0	0.05	36	87	39.2	10.4	50.4	0	17.9
0.4	0.05	35	84	39.1	11.3	49.6	0	17.5
5.1	0.05	34.4	85	39.3	11.4	49.3	0	17.4
18	0.05	34.4	84	42.0	11.0	47.0	0	18.2
20	0.24							
24	0.24	38.0	87	44.1	8.9	47.1	0	20.1
25	0.24	36.8	87	46.5	8.8	44.7	0	20.4
43	0.24	32.2	69	49.5	4.9	28.6	17	17.5
67	0.24	31.0	67	49.0	4.5	27.8	18.7	16.6
68	0.00							
69	0.00	33.8	80	50.8	5.4	30.2	13.6	19.0
76	0.00	36.7	83	50.3	5.9	33.0	10.8	20.6
82	0.00	35.9	83	50.4	6.4	34.2	9.0	20.4
90	0.00	36.3	85	49.7	6.9	36.2	7.1	20.5

[a] The catalyst had already been on stream for 150 h prior to starting this experiment.

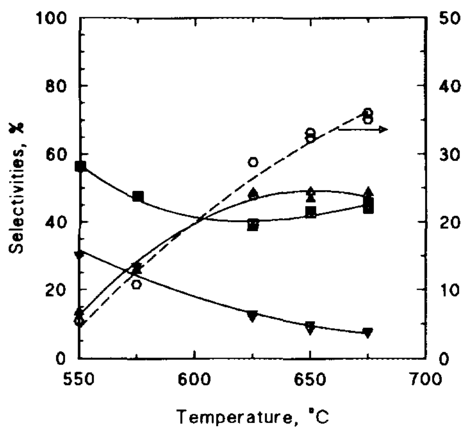

FIG. 2. Oxidative coupling of CH_4 over Li^+-MgO-Cl^- (1.0): (○) CH_4 conversion; (▲) C_2H_4, (▼) C_2H_6, and (●) CO_x selectivities. The reaction was carried out over 7.5 g catalyst (volume, 7.7 ml) with 60 Torr CH_4 and 30 Torr O_2 at 50 ml min^{-1}.

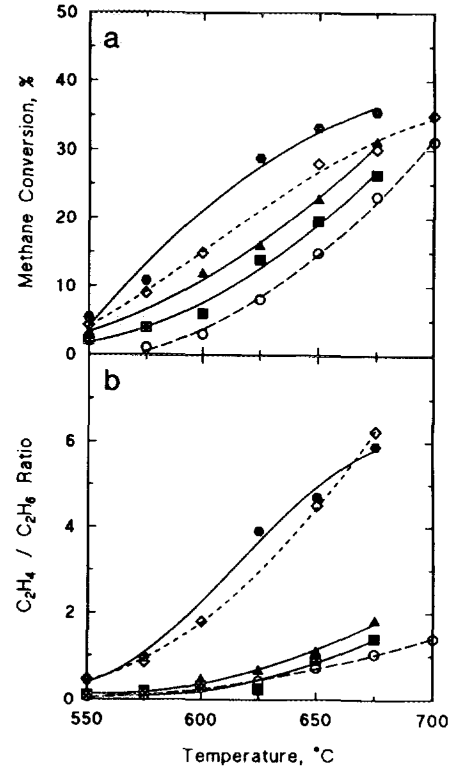

FIG. 3. Effect of Cl/Li ratio on (a) CH_4 conversion and (b) C_2H_4/C_2H_6 ratio: (●) Li^+-MgO-Cl^- (1.0), (▲) Li^+-MgO-Cl^- (0.7), (■) Li^+-MgO-Cl^- (0.3), (◇) Li^+-MgO-Cl^- (SG), (○) Li^+-MgO. The reaction was carried out with 60 Torr CH_4 and 30 Torr O_2 at a space velocity of 388 h^{-1}.

a space velocity of 388 h^{-1}. At these lower temperatures, the chlorine and the lithium were lost from the catalysts rather slowly. Results reported previously for the Li-MgO-Cl^- (SG) catalyst were similar (14), which demonstrates that the catalysts prepared by the two methods are functionally the same.

The Cl/Li ratio, however, has a marked effect on these catalysts, as shown by the results of Fig. 3, where CH_4 conversions and C_2H_4/C_2H_6 ratios are compared for four chlorine-containing catalysts and a Li^+-MgO catalyst. It is evident that the CH_4 conversion increases with Cl^- content, although not exactly in a linear manner because at the larger conversions, the system became oxygen limited. The most dramatic difference is found in the large increase in C_2H_4/C_2H_6 ratio that occurs at Cl/Li $\simeq$ 1. Comparable results have been obtained for the ethane OXD reaction in that the C_2H_6 conversion reached a maximum value at Cl/Li $\simeq$ 1 (22). Thus, surface chloride either modifies existing active centers in some manner or creates new centers that are especially active for the OXD of ethane. Subsequently, calcined catalysts that had Cl/Li ratios near unity (i.e., >0.9) are referred to as "good catalysts"; others are referred to as "poor catalysts".

Kinetic Results

Kinetic data were obtained under nearly differential conditions (O_2 conversion less than 20%) for a Li^+-MgO-Cl^- catalyst that had Cl/Li = 1.0. The CH_4 conversion increased linearly with respect to the 0.6 power of the O_2 pressure, as shown in Fig. 4. The most remarkable feature is that the catalyst was *not poisoned by the addition of CO_2*. Almost all oxidative coupling catalysts are strongly basic oxides, and they are severely poisoned by CO_2. For example, as shown in Fig. 5, the Li^+-MgO catalyst was poisoned both by CO_2 produced during reaction and by addition of CO_2 to the reagents. It was first pointed out by Ross and co-workers (23) that this poisoning has a strong effect on the apparent kinetics of the reaction, because as more O_2 is added, more CO_2 is produced. This phenomenon results in the curvature

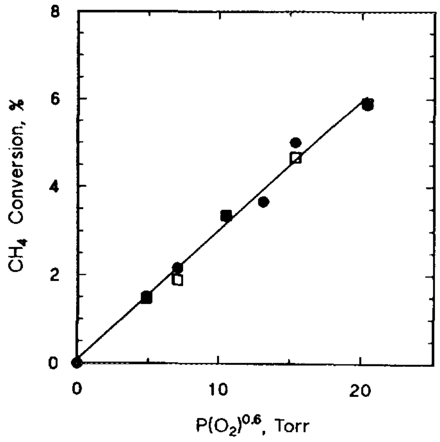

FIG. 4. Order of CH_4 reaction with respect to O_2 over the Li^+-MgO-Cl^- (1.0) catalyst at 650°C: (●) without addition of CO_2, (□) with addition of 6 Torr CO_2. The reaction was carried out over 0.2 g catalyst with 295 Torr CH_4 at a total flow rate of 50 ml min^{-1}; Li/Mg/Cl = 0.46/1.00/0.45.

shown in Fig. 5. By adding CO_2, one can make the reaction pseudo-zero-order in CO_2 and thereby obtain true kinetic data, but only on a severely poisoned catalyst. Ross and co-workers (24) found that the coupling reaction over a Li^+–MgO catalyst at 750°C was first order with respect to O_2, whereas, at 650°C we find nearly 0.8 order. When the addition of CO_2 was stopped, the catalyst regained its original activity, demonstrating the reversibility of the poisoning effect. It is, of course, much more straightforward to obtain the order of reaction for a good Li^+–MgO–Cl^- catalyst, since it is not poisoned by CO_2. The variations in CH_4 conversion with respect to the CH_4 pressure are shown in Fig. 6 for the Li^+–MgO–Cl^- and Li^+–MgO catalysts.

We have developed a heterogeneous–homogeneous model which adequately describes the orders of reactions (17). The model, which previously was applied to the kinetic data of Ross and co-workers (24), has been used to interpret the present results. The heterogeneous part of the mechanism is the same as that proposed previously for the oxidative coupling reaction (25), viz.

$$CH_4 + O_s^- \xrightarrow{k_1} CH_3\cdot + OH_s^- \qquad [1]$$

$$2OH_s^- \xrightarrow{k_2} H_2O + \square + O_s^{2-} \qquad [2]$$

$$\frac{1}{2}O_2 + \square + O_s^{2-} \underset{k_{-3}}{\overset{k_3}{\rightleftarrows}} 2O_s^- . \qquad [3]$$

Here, the active form of oxygen (e.g., O^- ions) must be modified by the presence of chlorine to the extent that it is no longer poisoned by CO_2. Based on kinetic isotope effect (KIE) studies (see below), we conclude that reaction [2] is rapid compared to the other reactions. In addition to these heterogeneous reactions, there are 156 gas phase reactions (18), but these play a relatively minor role in the conversion of CH_4 at 650°C.

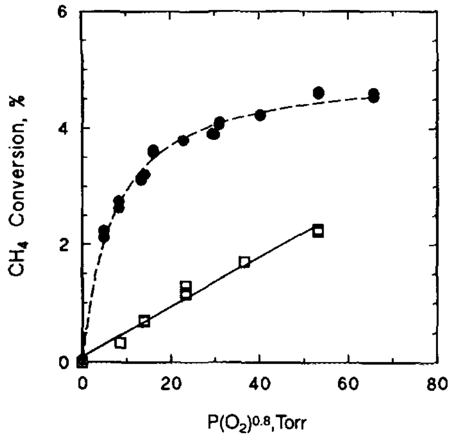

FIG. 5. Order of CH_4 reaction with respect to O_2 over the Li^+–MgO catalyst at 650°C: (●) without addition of CO_2, (□) with addition of 6 Torr CO_2. The reaction was carried out over 1.3 g catalyst with 295 Torr CH_4 at a total flow rate of ml min^{-1}.

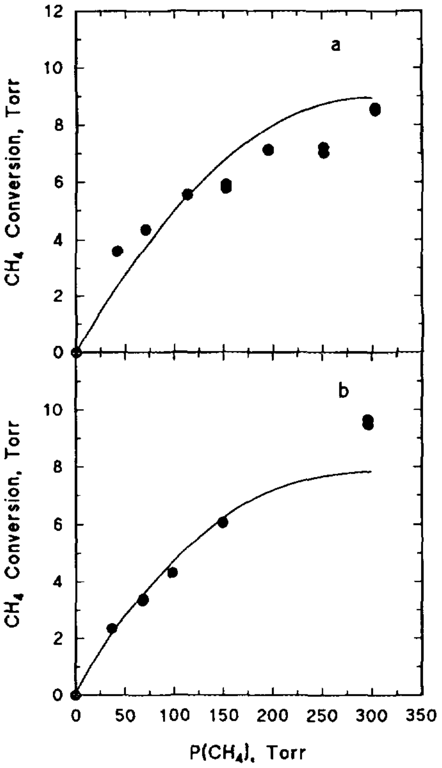

FIG. 6. Order of CH_4 reaction with respect to CH_4 over (a) Li^+–MgO–Cl^- (1.0) and (b) Li^+–MgO catalysts at 650°C. The reactions were carried out over 0.15 g Li^+–MgO–Cl^- (1.0) and 1.3 g Li^+–MgO with 50 Torr O_2 at a total flow rate of 50 ml min^{-1}; Li/Mg/Cl = 0.46/1.00/0.45.

According to this model, the orders of reaction are determined mainly by the forward and reverse rates of reaction [3] relative to the rate of reaction [1]. As the rate constants k_3 and k_{-3} increase at constant k_1 and k_3/k_{-3} ratio, the order becomes 1 with respect to O_2 and a fractional order with respect to CH_4. These values agree with the high-temperature results of Ross and co-workers (24). As k_3 and k_{-3} decrease, with k_3/k_{-3} and k_1 being held constant, the order with respect to O_2 decreases and the order with respect to CH_4 increases.

The solid lines of Figs. 4–6 were calculated using a particular set of the rate constants k_1, k_3, and k_{-3}. Over the Li^+–MgO–Cl^- (1.0) catalyst, the corresponding orders with respect to O_2 and CH_4 were 0.61 and 0.79, respectively, while over the Li^+–MgO catalyst, the corresopnding orders were 0.81 and 0.61. The fit to the data of Fig. 6b is not optimum, probably because the poisoning effect of CO_2 has not been accounted for. In this experiment, CO_2 was not added to the system. Qualitatively, our ability to fit the data with the model suggests that the rate of active oxygen formation and decomposition,

TABLE 3

Kinetic Isotope Effects Determined during the Oxidative Coupling of Methane[a]

Run No.	CH_4/O_2 = 2	CH_4/O_2 = 9
	Li^+-MgO-Cl^-	
1	1.70	1.87
2	1.74	1.79
3	1.76	1.89
4	1.67	1.79
5	1.69	1.81
Averaged and corrected[b]	1.55	1.66
	Li^+-MgO	
6	1.76	1.43
7	1.70	1.35
Averaged and corrected[b]	1.57	1.26

[a] T = 650°C, P (CH_4) = 180 Torr, 0.30 g of catalysts.

[b] Corrected by a factor of 1.1 for methyl radical collisions.

relative to the rate of hydrogen atom abstraction, determines the order of reaction.

The KIE results, obtained by simultaneously reacting CH_4 and CD_4 over the catalysts and measuring the distribution of H and D in the resulting ethane product, indicate that reaction [3] is comparable in rate to reaction [1]. As shown in Table 3, corrected KIE's of 1.55 and 1.57 were obtained for the Li^+-MgO-Cl^- (1.0) and Li^+-MgO catalysts, respectively, at $CH_4/O_2 = 2$ and 650°C. If the C-H bond breaking step were strictly rate-limiting, the theoretical KIE would have been about 1.84. Curiously, when the CH_4/O_2 ratio was increased to 9, the KIE increased to 1.66. Based on the proposed mechanism, one would have expected the forward rate of reaction [3] to have decreased realtive to reaction [1], giving a smaller KIE. The normal behavior was found with the Li^+-MgO catalyst at the larger CH_4/O_2 ratio. A KIE for reaction [2] was determined by first saturating CH_4 and O_2 with H_2O or D_2O and then carrying out the oxidative coupling reaction. No isotope effect was observed; therefore, we conclude, as did Cant *et al.* (26), that reaction [2] is not a rate-limiting step.

The apparent activation energy for the conversion of CH_4 over the Li^+-MgO-Cl^- (1.0) catalyst varied from 27 to 33 kcal mol^{-1}, depending on the CH_4/O_2 ratio. Unlike the case with the Li^+-MgO catalyst, for which apparent activation energies as large as 55 kcal mol^{-1} have been observed (24), the E_a's determined for Li^+-MgO-Cl^- are not dominated by CO_2 poisoning.

Although it is known that the large C_2H_4/C_2H_6 ratios result from the exceptional activity of the Li^+-MgO-Cl^- catalyst for the OXD of C_2H_6 (3), a comparative study of the rates of reaction for the three relevant hydrocarbons has not been previously carried out. The specific rates for the conversion of CH_4, C_2H_6, and C_2H_4 are compared in Table 4 for Li^+-MgO-Cl^- (1.0) and Li^+-MgO catalysts containing 4 wt% Li. Assuming that the reaction sequence can be approximated by $CH_4 \rightarrow C_2H_6 \rightarrow C_2H_4 \rightarrow CO_x$, to attain large C_2H_4/C_2H_6 ratios, it is required that the C_2H_6 be rapidly reacted to C_2H_4, and that the conversion of C_2H_4 be slow. Recent results using ^{13}C-labeled C_2H_4 have confirmed that ethylene is a major source of CO_2 over these catalysts, even at the relatively mild temperature of 650°C (27). From the information in Table 4, it is evident that the ratios of C_2H_6-to-CH_4 reaction rates are 1.5–1.8 greater for the Li^+-MgO-Cl^- catalyst than for the Li^+-MgO catalyst. Moreover, in all but the last entry, the reaction rates for C_2H_4 conversion were less over the Li^+-MgO-Cl^- catalyst. The interpretation of the results with respect to oxidative coupling are qualitative, however, because during the coupling reaction all three hydro-

TABLE 4

Relative Rates of Conversion for Methane, Ethane, and Ethylene[a]

Catalyst	Temp. (°C)	Flow rate, (cm^3 s^{-1})	Relative rates (µmol m^{-2} s^{-1}) Methane	Ethane	Ethylene	Rate C_2H_6 react./Rate CH_4 react.
Li^+-MgO	625	0.83	0.57	0.98	0.76	1.7
(SA = 0.58 m^2 g^{-1})	625	1.67	0.71	1.70	1.04	2.4
	650	0.83	1.01	2.26	1.83	2.2
	650	1.67	1.37	3.24	2.10	2.4
Li^+-MgO-Cl^- (1.0)	625	0.83	0.50	1.56	0.59	3.1
(SA = 3.2 m^2 g^{-1})	625	1.67	0.56	2.04	0.73	3.6
	650	0.83	0.89	3.35	1.19	3.8
	650	1.67	1.21	4.22	2.17	3.5

[a] 200 Torr of hydrocarbon, 100 Torr of oxygen, balance was helium; 0.7 g Li^+-MgO, 0.3 g Li^+-MgO-Cl^-; the space velocities were equivalent.

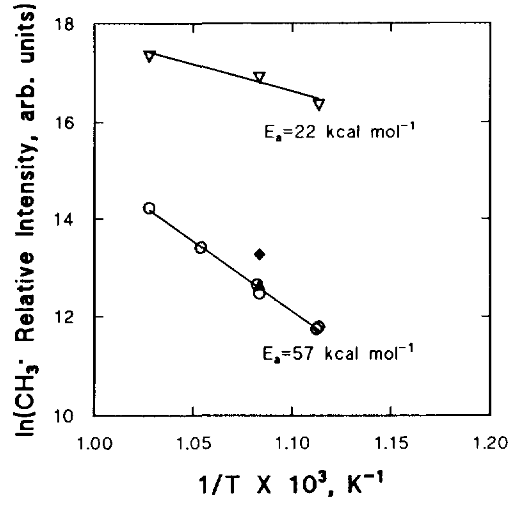

FIG. 7. Methyl radical formation over (▽) Li^+–MgO and (○) Li^+–MgO–Cl^- (1.0) catalysts; after addition of 1.5 Torr CO_2 to the reactants over (◆) Li^+–MgO and (▲), Li^+–MgO–Cl^- (1.0). The total pressure was ca. 2 Torr over 0.15 g of each catalyst.

carbons would compete for the same set of active centers, with ethane being favored as a result of its weaker C–H bond. Therefore, in reality, the competitive rates would favor the C_2H_6 reaction even more than is indicated in Table 4.

The results obtained at different flow rates show that the larger reaction rates were obtained at the larger flow rates. In part, this reflects the fact that the product molecules, including CO_2 for the Li^+–MgO catalyst, compete for the active centers. We have no explanation for the larger values obtained during the oxidation of C_2H_4 over the Li^+–MgO–Cl^- catalyst, as there were no hydrocarbon products and CO_2 does not poison the catalyst.

In comparing the activities of the two catalysts, one should note that the surface area of the Li^+–MgO–Cl^- catalyst was 5.5 times greater than that of the Li^+–MgO catalyst. Thus, on a per-gram basis, the chlorided catalyst would be 7 times more active than the Li^+–MgO catalyst for C_2H_6 conversion. Previously, it was shown (3) that the percentage of C_2H_6 conversion, under integral conditions, was 2.7 times greater over a Li^+–MgO–Cl^- (SG) catalyst than over a Li^+–MgO catalyst.

Methyl Radical Formation

Surface-generated gas-phase $CH_3\cdot$ radicals were detected using the matrix isolation electron spin resonance (MIESR) system described previously (28). Arrhenius plots of $CH_3\cdot$ radical production, both with and without added CO_2, are shown in Fig. 7. These results were obtained at an O_2 pressure over the catalyst of about 0.01 Torr; therefore, the pressure of CO_2 resulting from the reaction was quite small. Under these conditions, E_a over the Li^+–MgO catalyst was ca. 22 kcal mol^{-1}, in good agreement with previously reported results (29). The surprising result was that the activity for $CH_3\cdot$ radical formation was so much greater over the Li^+–MgO catalyst than over the Li^+–MgO–Cl^- catalyst. When 1.5 Torr of CO_2 was added to the reagents, the Li^+–MgO catalyst was severely poisoned, but, as expected, the Li^+–MgO–Cl^- catalyst was unaffected. As a result, after CO_2 addition the two catalysts had comparable activities for $CH_3\cdot$ radical generation.

The E_a of 57 kcal mol^{-1} for $CH_3\cdot$ radical formation over Li^+–MgO–Cl^-, obtained in the low pressure mode ($P_{\text{Total}} \approx 2$ Torr), is considerably greater than the values of 27–33 kcal mol^{-1} that were found in the conventional reactor. When the MIESR system was operated at 760 Torr with 203 Torr CH_4 and 25 Torr O_2, the E_a was 35 kcal mol^{-1}. The larger value of 57 kcal mol^{-1} may result from a change in the rate-limiting step in the catalytic cycle when the partial pressure of O_2 was only 0.01 Torr.

TPD of CO_2

The TPD results for the three Li^+–MgO–Cl^- (*ex.* HCl) catalysts and the Li^+–MgO catalyst of Fig. 3 are depicted in Fig. 8. The amount of CO_2 that was held on the catalysts, presumably as carbonate ions, decreased with increasing chloride content, until at Cl/Li = 1 the amount of CO_2 desorbed was very small ($\approx$ 0.001 CO_2/Li). For the Li^+–MgO sample, the molar CO_2/Li ratio was 0.16. Apparently, much of the Li^+ on the surface is present as an oxide or as a hydroxide. The small amount of CO_2 held on the Li^+–MgO–Cl^- (1.0) catalyst is consistent with the observation that CO_2 did not poison this material. The presence of chlorine causes not only a decrease in the amount of adsorbed CO_2, but also a shift in the desorption

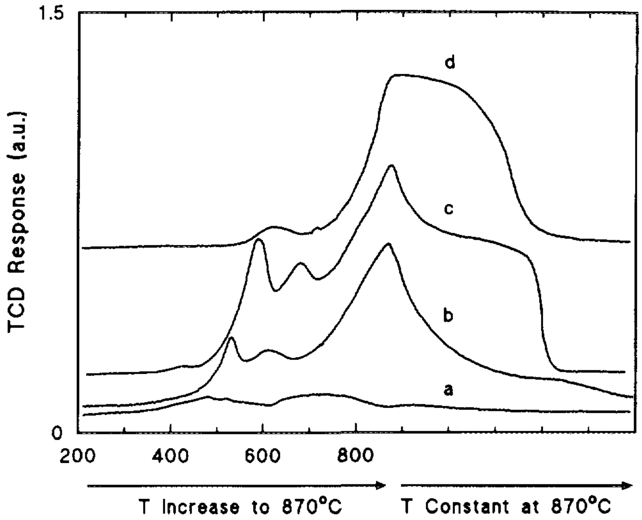

FIG. 8. TPD of CO_2 from catalysts: (a) Li^+–MgO–Cl^- (1.0), (b) Li^+–MgO–Cl^- (0.7), (c) Li^+–MgO–Cl^- (0.3), (d) Li^+–MgO. The amounts of catalysts used were 130 mg for (a)–(c) and 65 mg for (d).

peak to lower temperatures. It should be emphasized that the peak at 870°C is not a true TPD maximum, as the temperature was ramped up to this value and then held constant. The variations in the amount of CO_2 and the shift to lower temperature maxima suggest that the presence of chloride ions decreases both the number of basic sites and the basic strength of these sites. Since the decomposition temperature of $MgCO_3$ is 420°C at a CO_2 pressure of 1 Torr, all of the peaks in Fig. 8 at $T > 500°C$ must be associated with lithium. Pure Li_2CO_3, however, exhibited a rather sharp decomposition peak at 733°C. One may conclude, therefore, that there is a synergism between Li^+ and MgO that gives rise to the several CO_2 TPD peaks. The dynamics of the adsorption–desorption process also may play a role in the width of the peaks and the temperature at which the maxima occur. For the Li^+–MgO sample, it is likely that the reversible catalyst poisoning at 650°C is associated with the TPD peak at ca. 600°C. In a separate experiment, it was shown that the TPD peaks shifted to a higher temperature when CO_2 was added to the He stream. Thus, in the presence of CO_2, the peak at 600°C could shift to approximately 650°C.

The TPD results described here for the Li^+–MgO–Cl^- catalysts are very different from those reported by Ruckenstein and Khan (15), who found that a large amount of CO_2 was strongly bound on a catalyst that had been prepared by the addition of LiCl to MgO. In their experiments, the CO_2 was adsorbed at 50°C and desorbed at progressively higher temperatures. We repeated this mode of adsorption and again found that almost no CO_2 was adsorbed on our good Li^+–MgO–Cl^- catalysts.

XRD of Catalysts

Evidence for the presence of certain phases on the catalysts was obtained by XRD. As expected from the TPD results, a Li_2CO_3 phase was clearly evident on the Li^+–MgO catalyst. By contrast, the fresh Li^+–MgO–Cl^- (SG) catalyst had a LiCl phase, in addition to MgO, but no Li_2CO_3 phase. After reaction, a trace amount of the carbonate phase may have existed. Similarly, a Li^+–MgO–Cl^- (1.0) catalyst exhibited only a LiCl phase after 231 h on stream, but no Li_2CO_3 phase. A catalyst having Cl/Li = 0.03 was characterized by a Li_2CO_3 phase; no LiCl phase was detected. These results demonstrate that when an adequate amount of Cl^- is present, the LiCl phase prevails, and the Li_2CO_3 phase is largely excluded.

SUMMARY AND CONCLUSIONS

The addition of Cl^- ions to a Li^+–MgO catalyst at a ratio of $Cl/Li \simeq 1$ has a remarkable effect on the activity for the reaction of C_2H_6 to C_2H_4. The presence of Cl^- ions significantly increases the rate of C_2H_6 conversion relative to the rate of CH_4 conversion. As a consequence, exceptionally large C_2H_4/C_2H_6 ratios are observed during the oxidative coupling of CH_4. Moreover, the presence of chloride ions limits the sintering of the catalyst, and prevents the poisoning of the catalyst by CO_2, which is a product of the reaction. Although the specific activities are similar, the CH_4 conversion levels, at a constant space velocity, are actually greater over a good Li^+–MgO–Cl^- catalyst than over a Li^+–MgO catalyst. The presence of Cl^- ions inhibits the formation of Li_2CO_3, which, if present in sufficient amount, essentially covers the surface of the catalyst. The latter observation is based on XPS results that will be described in a subsequent paper in this series (22).

From results described to this point, one might conclude that at a certain Cl/Li ratio, a LiCl phase is formed, and this phase is responsible for the catalytic conversion of CH_4 and/or C_2H_6. However, the XPS and additional XRD data will demonstrate that the differences between good catalysts with $Cl/Li \geq 0.9$ and poor catalysts with $Cl/Li < 0.9$ are subtle and cannot be explained by the presence or absence of LiCl on the surface.

The different decay patterns for CH_4 conversion and C_2H_4 productivity indicate that two different types of active centers are operative on the Li^+–MgO–Cl^- catalysts. One type is responsible for the activation of CH_4 and C_2H_6, while another type is responsible for the activation of only C_2H_6. It should be recalled that the C–H bond strengths in CH_4 and C_2H_6 are 104 and 98 kcal mol^{-1}, respectively; thus, it should be easier to activate C_2H_6. The nature of the active centers remains a matter of speculation; however, it is clear that Cl^- ions either create new centers or they make the existing ones on Li^+–MgO less basic, so that they are not poisoned by CO_2.

ACKNOWLEDGMENT

This research was supported by the Gas Research Institute under Contract 5086-260-1326.

REFERENCES

1. Burch, R., and Tsang, S. C., *Appl. Catal.* **65,** 259 (1990).
2. Ahmed, S., and Moffat, J. B., *Appl. Catal.* **58,** 83 (1990).
3. Conway, S. J., and Lunsford, J. H., *J. Catal.* **131,** 513 (1991).
4. Burch, R., Squire, G. D., and Tsang, S. C., *Appl. Catal.* **46,** 69 (1989).
5. Baldwin, T. R., Burch, R., Crabb, E. M., Squire, G. D., and Tsang, S. C., *Appl. Catal.* **56,** 219 (1989).
6. Burch, R., Crabb, E. M., Squire, G. D., and Tsang, S. C., *Catal. Lett.* **2,** 249 (1989).
7. Otsuka, K., Hatano, M., and Komatsu, T., *Catal. Today* **4,** 409 (1989).
8. Warren, B. K., *Catal. Today* **13,** 311 (1992).
9. Moggridge, G. D., Rayment, T., and Lambert, R. M., *J. Catal.* **134,** 242 (1992).
10. Burch, R., Chalker, S., and Loader, P., *in* "Proceedings, 10th Inter-

national Congress on Catalysis, Budapest, 1992" (L. Guczi, F. Solymosi, and P. Tetenyi, Eds.), p. 174. Akadémiai Kiadó, Budapest, 1993.

11. Thomas, J. M., Ueda, W., Williams, J., and Harris, K. D. M., *Faraday Discuss. Chem. Soc.* **87,** 33 (1989).
12. Khan, A. Z., and Ruckenstein, E., *Catal. Lett.* **13,** 95 (1992).
13. Otsuka, K., Liu, Q., Hatano, M., and Mariawa, A., *Chem. Lett.* 486 (1986).
14. Hinson, P. G., Clearfield, A., and Lunsford, J. H., *J. Chem. Soc., Chem. Commun.,* 1430 (1991).
15. Ruckenstsein, E., and Khan, A. Z., *Catal. Lett.* **18,** 27 (1993).
16. Khan, A. Z., and Ruckenstein, E., *J. Catal.* **139,** 304 (1993).
17. Shi, C., Hatano, M., and Lunsford, J. H., *Catal. Today* **13,** 191 (1992).
18. Shi, C., Xu, M., Rosynek, M. P., and Lunsford, J. H., *J. Phys. Chem.* **97,** 216 (1993).
19. Yamaguchi, O., Tonami, H., Hayashi, T., and Shimizu, K., *J. Jpn. Soc. Powder Met.* **24,** 157 (1976).
20. Yamaguchi, O., Tonami, H., and Shimizu, K., *Chem. Lett.* 799 (1976).
21. Hutchison, D., and Jeffery, P. G., "Chemical Methods of Rock Analysis," 3rd ed., p. 138. Pergammon, New York, 1981.
22. Wang, D.-J., Rosynek, M. P., and Lunsford, J. H., in press.
23. Korf, S. J., Roos, J. A., deBruijin, N. A., van Ommen, J. G., and Ross, J. R. H., *J. Chem. Soc., Chem. Commun.,* 1433 (1987).
24. Roos, J. A., Korf, S. J., Vehof, R. H. J., van Ommen, J. G., and Ross, J. R. H., *Appl. Catal.* **52,** 131 (1989).
25. Ito, T., Wang, J.-X., Lin, C.-H., and Lunsford, J. H., *J. Am. Chem. Soc.* **107,** 5062 (1985).
26. Cant, N. W., Lukey, C. A., Nelson, P. F., and Tyler, R. J., *J. Chem. Soc., Chem. Commun.,* 766 (1988).
27. Shi, C., Rosynek, M. P., and Lunsford, J. H., unpublished results.
28. Martir, W., and Lunsford, J. H., *J. Am. Chem. Soc.* **103,** 3728 (1981).
29. Xu, M., Shi, C., Yang, X., Rosynek, M. P., and Lunsford, J.H., *J. Phys. Chem.* **96,** 6395 (1992).